Fourier Transform Infrared Spectroscopy Provides a Fingerprint for the Tetramer and for the Aggregates of Transthyretin

Yraima Cordeiro,* Julia Kraineva,† Marisa Carvalho Suarez,* Anna Gabriella Tempesta,* Jeffery W. Kelly,‡ Jerson L. Silva,* Roland Winter,† and Debora Foguel*

*Instituto de Bioquímica Médica, Programa de Biologia Estrutural, Universidade Federal do Rio de Janeiro, RJ 21941-590, Brazil; †Department of Chemistry, Physical Chemistry I, University of Dortmund, D-44227 Dortmund, Germany; ‡The Scripps Research Institute, La Jolla, California 92037

ABSTRACT Transthyretin (TTR) is an amyloidogenic protein whose aggregation is responsible for several familial amyloid diseases. Here, we use FTIR to describe the secondary structural changes that take place when wt TTR undergoes heat- or high-pressure-induced denaturation, as well as fibril formation. Upon thermal denaturation, TTR loses part of its intramolecular β-sheet structure followed by an increase in nonnative, probably antiparallel β-sheet contacts (bands at 1616 and 1686 cm^{-1}) and in the light scattering, suggesting its aggregation. Pressure-induced denaturation studies show that even at very elevated pressures (12 kbar), TTR loses only part of its β-sheet structure, suggesting that pressure leads to a partially unfolded species. On comparing the FTIR spectrum of the TTR amyloid fibril produced at atmospheric pressure upon acidification (pH 4.4) with the one presented by the native tetramer, we find that the content of β-sheets does not change much upon fibrillization; however, the alignment of β-sheets is altered, resulting in the formation of distinct β-sheet contacts (band at 1625 cm^{-1}). The random-coil content also decreases in going from tetramers to fibrils. This means that, although part of the tertiary- and secondary-structure content of the TTR monomers has to be lost before fibril formation, as previously suggested, there must be a subsequent reorganization of part of the random-coil structure into a well-organized structure compatible with the amyloid fibril, as well as a readjustment of the alignment of the β-sheets. Interestingly, the infrared spectrum of the protein recovered from a cycle of compression-decompression at pD 5, 37°C, is quite similar to that of fibrils produced at atmospheric pressure (pH 4.4), which suggests that high hydrostatic pressure converts the tetramers of TTR into an amyloidogenic conformation.

INTRODUCTION

Transthyretin (TTR) is a tetrameric protein composed of identical 127-residue subunits having a predominantly β-sheet structure (1). The eight strands present in TTR are organized into two β-sheets (DAGH and CBEF). TTR is found in human plasma (0.1–0.4 mg/mL) and cerebral spinal fluid (0.017 mg/mL) (2). The plasma form serves as a secondary carrier for thyroxin and for binding retinol-binding protein (3–5). Wild-type (wt) TTR is responsible for senile systemic amyloidosis, a disease that affects 25% of people over 80 years old, and is characterized by heavy amyloid deposits in the heart (6,7). On the other hand, more than 100 point mutants of TTR have been described thus far, most of them involved in familial amyloidotic polyneuropathy (FAP) and familial amyloidotic cardiomyopathy (8). In general, FAP patients present the first symptoms by the second or third decade with peripheral neuropathy, cardiomyopathy, carpal tunnel syndrome, and vitreous opacities (9,10).

Several thermodynamic and kinetic studies have been performed with wt and variants of TTR to correlate their thermodynamic stability with their amyloidogenicity (11–14). Recently, an elegant study by Sekijima and co-workers evaluated the energetic and secretion efficiency of wt and 32 variants of TTR by mammalian cells, showing that thermodynamic and kinetic stability have to be considered together to explain TTR secretion efficiency that ultimately leads to aggregation (15).

Most studies that have evaluated TTR aggregation have used low pH (3.5–5.0), where TTR undergoes dissociation and partial unfolding before aggregation (11,16,17). Chemical denaturing agents such as urea and guanidine hydrochloride have also been used, showing the great stability of wt TTR as well as its slow dissociation-unfolding constant (16,18–20). There are very few thermal-denaturation studies with TTR (21,22).

Another tool that has been used successfully to investigate the unfolding of several proteins, including TTR, is high hydrostatic pressure (HHP) (23–26). HHP has an advantage over other methods because its perturbation of macromolecules in solution depends solely on the volume change of the process under study with no perturbation by the thermal energy of the system (23,25). HHP favors the formation of structures with lower volumes, and application of pressure generally hydrates the hydrophobic core of the proteins, melting mainly their tertiary structure (25,27). This makes HHP a tool suitable for trapping partially folded states of proteins.

Submitted March 27, 2006, and accepted for publication May 4, 2006.

Y. Cordeiro and J. Kraineva contributed equally to this work.

Address reprint requests to Debora Foguel, Instituto de Bioquímica Médica, Universidade Federal do Rio de Janeiro, Av. Bauhínia 400, Bloco E S42, Rio de Janeiro, 21941-590, RJ, Brazil. Tel.: 55-21-2562-6761; Fax: 55-21-3881-4155; E-mail: foguel@bioqmed.ufrj.br.

0006-3495/06/08/957/11 $2.00

doi: 10.1529/biophysj.106.085928

In previous studies performed by our group and Akasaka's, the unfolding of TTR (wt and variants) was investigated by the use of HHP, where the changes in fluorescence or NMR were employed to assess the thermodynamic parameters associated with its unfolding (14,28,29). More recently, Heremans and collaborators have used Fourier transform infrared spectroscopy (FTIR) and atomic force microscopy (AFM) to investigate the stability against high pressure of amyloid fibrils formed by a small TTR peptide ($TTR_{105–115}$) (30). They observed that early $TTR_{105–115}$ aggregates were dissociated by relatively low pressures, whereas mature aggregates were highly pressure resistant (30); a similar result was observed by our group with prion protein aggregates (31).

Here we compare the pressure- and thermal-induced unfolding of wt TTR using FTIR to probe the changes in the secondary structure of TTR. The experiments were performed at pD 7.5 or 5.0 due to the fact that TTR spends most of its lifetime at neutral pH found in blood and because, as shown before, at acidic pH (<5), TTR assumes an amyloidogenic conformation that can evolve into fibrils (11,13, 16,18,32). The secondary-structure content of wt TTR calculated from the FTIR spectra is almost identical to that calculated from the crystal structure (44% β-sheet; 3.1% α-helix; 29.5% random coil; and 23.4% turns). Upon heating, TTR undergoes denaturation only at very high temperatures (>80°C), confirming its high thermodynamic stability (22,29,33). However, when the temperature returns to 20°C, the protein forms aggregates with a high content of nonnative (probably antiparallel) β-sheet contacts and a lower content of native, intramolecular β-sheets. As expected, the heat-induced aggregation is greater at pH 5.0 than at pH 7.5. When subjected to HHP, part of the β-sheet of TTR is lost in the pressure range of 1–3 kbar, regardless of the pH employed. However, when the pressure titration is performed at 5°C, the changes in the secondary structure are shifted to lower pressure values. These data reinforce the importance of hydrophobic interactions to TTR stability. Strikingly, after pressure release, at pD 5.0, 37°C, the recovered FTIR spectrum resembles that of the amyloid fibril of TTR produced at atmospheric pressure at pH 4.4. These data are in accordance with our previous observations showing that after a cycle of compression-decompression at pH 5.0, TTR forms fibrils that bind Congo red and thioflavin T (28,29). The amyloid fibril of TTR produced either by acidification (pH 4.4) or after HHP treatment at pD 5.0 presents a similar β-sheet profile, which is significantly distinct from the one observed after heat treatment. Surprisingly, the β-sheet content of the soluble protein is quite similar to that of the amyloid fibrils (~45%).

In this study, we present a complete description of the changes in the secondary-structure content of wt TTR that take place when the protein is heat or pressure denatured. Other techniques that evaluate the secondary structure of proteins, such as circular dichroism (CD), are unable to distinguish between these forms, one of them soluble and ordered (fibrils) and the other a disordered aggregate.

MATERIAL AND METHODS

Samples

Recombinant human TTR was expressed and purified as described (32) and lyophilized afterward to completely remove H_20 from the samples. The experiments were performed at two different pD values, 7.5 and 5.0. After deuterium substitution of solvent-exposed fast-exchanging amide protons, TTR was dissolved in 99.9% D_2O at a concentration of 4% (wt/wt) in 10 mM Tris buffer (pD 7.5) or in 10 mM MES (2-(*N*-morpholino)-ethanesulphonic acid) buffer (pD 5.0) for all high-pressure measurements. The temperature-insensitive phosphate buffer 10 mM, pD 7.0, was used for the temperature scans. All buffers utilized were supplemented with 100 mM KCl. Throughout all experiments, only fresh samples were used. All chemicals, apart from TTR, were purchased from Sigma-Aldrich (Munich, Germany).

The amyloid fibrils of TTR were produced by incubating 10 μM protein at 37°C for 72 h in 25 mM acetate, 100 mM KCl, pH 4.4, without stirring.

Fourier transform infrared spectroscopy

For the temperature-dependence studies, protein solutions were injected into an infrared cell with 4-mm thick CaF_2 windows separated by 50-μm mylar spacers. The temperature in the cell was controlled by an external water circuit and was increased gradually between 20°C and 100°C at 20°C per h scan rate. A diamond anvil cell was used for the pressure-dependence studies (High Pressure Diamond Optics, Tucson, AZ). The samples were placed together with powdered α-quartz in a 0.50-mm diameter hole of a 50-μm-thick stainless steel gasket (34), and changes in pressure were quantified by the shift of the phonon band of quartz at 798 cm^{-1}. The pressure-dependence studies were carried out between 1 bar and ~12 kbar. An equilibration time of ~15 min was ensured before the spectra were collected at each temperature and pressure, hence leading to an increase of pressure at a rate of ~2 kbar/h. The FTIR spectra were also collected up to 18 h after decompression to ambient pressure (1 atm) or after return to room temperature (25°C).

The FTIR spectra were collected on a Nicolet (Madison, WI) Magna 550 FTIR spectrometer equipped with a mercury cadmium telluride detector operated at −196°C. Spectra were generated by coadding 256 interferograms collected at 2-cm^{-1} resolution and apodized with a Happ-Genzel function. As background, the respective spectrum of buffer in D_2O was used. The sample chamber was purged with dry, CO_2-free air. Determination of peak position and curve fitting were performed with the OMNIC (Nicolet) and GRAMS (Galactic, Salem, NH) software, respectively. Integral intensities of the secondary-structure elements were calculated by analysis of the amide I′ (the prime indicates that the solvent is D_2O) vibration mode of the infrared spectrum (35). Fourier self-deconvolution of the infrared (IR) spectra was performed with a resolution enhancement factor of 1.8 and a bandwidth of 15 cm^{-1}. The deconvoluted amide I′ spectrum was then decomposed into subbands using mixed Gaussian-Lorentzian functions (31,36), and the relative peak areas (integral intensities) of all secondary-structure elements revealed were determined. In fact, the peak positions obtained from the analysis are in good agreement with previous peak assignments. In addition, we have compared our results on the population of secondary-structure elements obtained by the FTIR data analysis with those deduced from the x-ray structure of the wt TTR (Protein Data Bank (PDB) 1F41), and good agreement has been found. We note that the results of this method need to be treated with caution for the determination of absolute values of the secondary-structure elements because their transition dipole moments may be different and because theoretical predictions of the absorbance frequencies of model polypeptide secondary structures showed that they may be influenced by structural distortions, variable (hydrogen/deuterium) H/D exchange, etc. No problems arise, however, from the application of the fitting method to the study of relative changes in conformations of the protein backbone, which was the primary goal of this study. The error in determination of the secondary-structure elements from the relative peak areas of the amide I′ band (integral intensities) from different runs is ~±2%.

Light-scattering measurements

Native tetramers (5 μM) were incubated in 10 mM MES, 100 mM KCl, pH 5.0. Then, the temperature was increased to 85°C, and the light scattered by the sample was recorded by exciting at 320 nm and collecting the scattered light from 315–325 nm in an ISS-PC spectrofluorometer (Champaign, IL). The extent of aggregation was evaluated by dividing the spectral area observed at any given temperature by the one observed at 25°C.

Far-ultraviolet circular dichroism spectroscopy

CD spectra of wt TTR under different oligomerization states, namely, tetramer, heat-induced aggregates, or acid-induced amyloid fibrils, were recorded using a Jasco J-715 spectropolarimeter (Jasco Corporation, Tokyo, Japan). All samples were examined at a concentration of 5 μM, although the precise concentrations of the heat-induced aggregates as well as amyloid fibrils could be lower due to some loss during their preparation. All CD spectra had the respective buffer spectra subtracted from them and were collected with four accumulations each in a 2.00-mm path length quartz cell.

RESULTS AND DISCUSSION

Analysis of the secondary-structure content of TTR by FTIR spectroscopy

The most useful IR band for the analysis of the secondary structure of proteins in aqueous media is the amide I band (which downshifts by ~5 cm^{-1} in D_2O as solvent and is then labeled amide I′ band), which appears between ~1700–1600 cm^{-1} (35). The amide I band represents 76% of the C=O stretching vibration of the amide group, coupled to the C-N stretching (14%) and C-C-N deformation (10%) mode. The exact frequency of this vibration depends on the nature of the hydrogen bonding involving the amide group, and this is determined by the particular secondary structure adopted by the protein. Using the method described in the Materials and Methods section, the component bands representing α-helices, β-sheets, turns, and random structures can be determined. The percentages of these structures are estimated by adding the areas of the component bands and then expressing the sum as a fraction of the total amide I′ band area. Due to the unknown transition dipole moments of the various secondary elements, no absolute values for the population of conformational states can be given; only relative changes can be obtained and are discussed.

Recently, Zandomeneghi and collaborators performed an elegant evaluation of the molecular structure of the amyloid fibrils of several different proteins whose FTIR spectra have already been published and compared them with the β-sheet content of their native proteins (37). TTR was one of the proteins evaluated. However, the authors did not present a detailed description of the secondary-structure content of TTR extracted from the FTIR spectrum (37). To our knowledge, there is no other report in the literature where FTIR has been used to quantify the changes in the secondary-structure content that take place upon denaturation and aggregation of TTR. This became our objective.

Fig. 1 *b* shows the FTIR spectrum of wt TTR in the soluble state at pD 7.5, 25°C. Curve-fitting of the amide I' spectrum revealed bands (Fig. 1 *b*) at ~1675 (turns/β-sheets), 1655 (α-helices), 1646 (random coil), 1634/1627 (β-sheets), and 1686/1616 (nonnative, aggregated β-sheets) cm^{-1}. Previous investigations suggested that FTIR might be able to distinguish between parallel and antiparallel β-sheets (38,39), since the latter possess amide I′ maxima at ~1616 and 1685 cm^{-1}, whereas the former reveals maxima at ~1626 cm^{-1}. However, in other studies it has been argued that these bands do not allow for a general discrimination between parallel and antiparallel β-sheets (35). Thus, here, we prefer to assign the band at 1627 cm^{-1} simply as β-sheet, and the ones at 1616 and 1685 cm^{-1} as nonnative, aggregated β-sheets (they

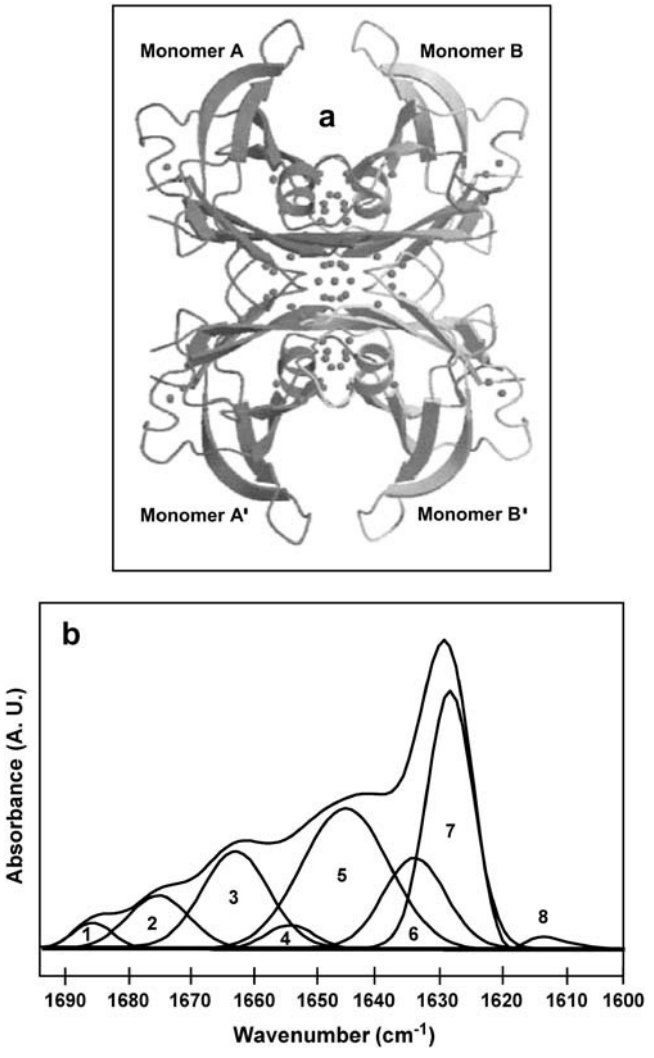

FIGURE 1 (*a*) X-ray structure of wt TTR (PDBfile 1F41) obtained at 1.5-Å resolution, showing the four monomers. (*b*) Secondary-structure analysis of wt TTR by FTIR. Curve fitting of the deconvoluted amide I′ band of wt TTR (37°C, pD 7.5) with eight Gauss-Lorentz functions: 1and 8, nonnative, aggregated β-sheets; 2 and 3, turns; 4, α-helices; 5, random coil; and 6 and 7, β-sheets.

were observed for the heat-induced aggregate only). According to the fitting of the amide I' band by the subcomponents described above, the average structure of the native protein at pD 7.5, 25°C contains 44% β-strands, 3.1% α-helix, 29.5% random coil, and 23.4% turns, with an accuracy of $\pm 2\%$ (Table 1). We recall that, strictly speaking, due to possible differences in the transition dipole moments of the secondary structures, these numbers do not give absolute values, but are proportional to their actual population. Hence, only their relative changes should be considered.

The x-ray structures of the wt (Fig. 1 *a*) as well as of several variants of TTR have already been solved, thus allowing us to quantify the secondary-structure elements of TTR (40). To validate our FTIR analysis, we compare the percentages of secondary-structure elements of TTR extracted from the FTIR spectrum (Fig. 1 *b*) with those obtained by x-ray analysis of the TTR crystal at 1.5-Å resolution (40) (PDB1F41) (Table 1).

The x-ray diffraction data yield 8 β-strands (A–H) in 2 β-sheets for each monomer, 1 α-helix, 10 β-turns, 2 γ-turns, 6 β-bulges, and 4 β-hairpins (40). Two monomers form a dimer whose contact interface is formed by extensive H-bonds between the two adjacent H (Ser-115–Thr-123) strands and F (Ala-91–Ala-97) strands from each monomer. The dimer-dimer interface involves the interaction between the AB (residues 19–28) and GH (residues 113–114) loops. As calculated from the PDB-file 1F41 for the monomers A and B in human TTR crystals, this amounts to 48% strands, 5.5% α-helices; and the remaining 46.5% consists of turns, hairpins, and random-coil structures (Table 1). These data were recalculated for a TTR tetramer consisting of 4×127 residues, assuming that the monomers do not change their final structure in the tetramer.

As seen in Table 1, there is a good correlation between the secondary structural content of TTR calculated from the x-ray data and from the FTIR spectrum reported here, which gives us confidence that FTIR can be used to evaluate changes in its secondary structure during heat- and high-hydrostatic-pressure- (HHP) induced denaturation with reasonable accuracy. It is worth remembering that, although CD measurements could be used to probe the changes in secondary structure of TTR during thermal-induced denaturation, at present it is not possible to perform such experiments under HHP due to the pressure-induced birefringence of the sapphire windows in commercial high-pressure cells. Besides, FTIR is a more precise technique than CD for evaluating the β-sheet content of proteins (35).

TABLE 1 Comparison of percentage of secondary-structure components obtained by FTIR with previous data from x-ray crystallography (PDB 1F41)

Secondary-structure component	Secondary structure calculated from x-ray data (PDB 1F41) (%)	Secondary structureat 25°C and pD 7.5calculated from FTIR (%)
β-sheets	48.0	44.0
Helices	5.5	3.1
Random coils	31.5	29.5
Turns	15.0	23.4

Thermal-induced denaturation of TTR as followed by FTIR

Having shown that the secondary-structure content calculated from the FTIR spectrum reasonably reflects the actual secondary-structure content of TTR, we performed thermal-denaturation studies evaluating the changes in the FTIR component bands (Fig. 2). The experiments were performed at pD 7.5 and 5.0. The effect of temperature (from 5°C to 100°C) on the secondary structure of TTR at pD 5.0 is shown in Fig. 2. The corresponding FTIR spectra and the relative integral intensities of subcomponents obtained upon heating

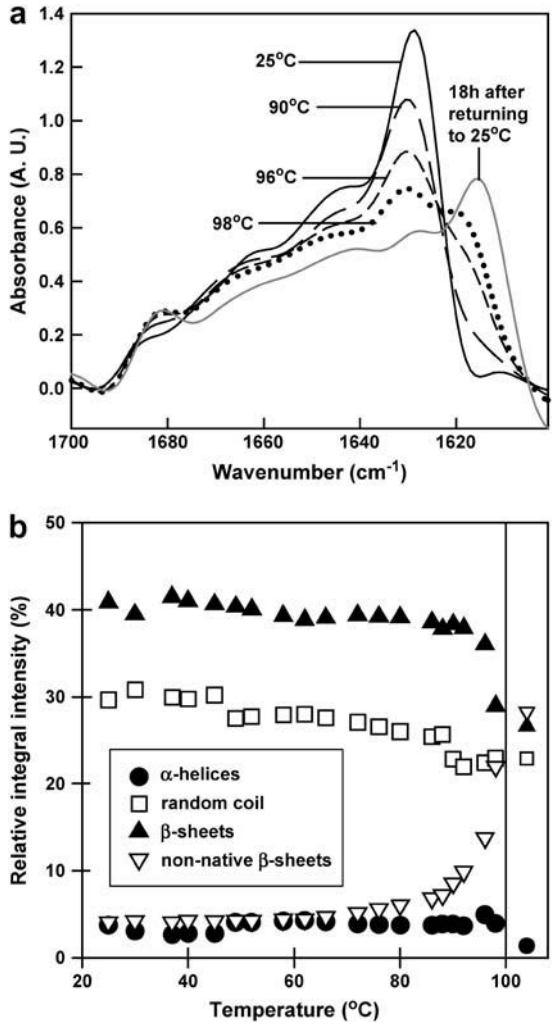

FIGURE 2 Temperature-induced unfolding of wt TTR. (*a*) FTIR spectra of 4% (w/w) wt TTR at pD 5.0 as a function of temperature increase (only selected temperatures are shown). (*b*) Relative intensities of wt TTR secondary-structure components as a function of increasing temperatures. The isolated symbols on the right correspond to the respective secondary-structure components after returning to 25°C.

at pD 7.5 are not shown due to their similarity to the data obtained at pD 5.

The maximum of the amide I′ band in the native protein occurs at ~1628 cm^{-1}, which is typical for β-sheet-rich proteins (Fig. 2 *a*) (35). In the study performed by Zandomeneghi and collaborators (37), native TTR exhibited an IR band with a maximum at 1630 cm^{-1}, in accordance with our study. The temperature-induced unfolding is indicated by a decrease of this band and a concomitant increase in two bands at 1616 and 1686 cm^{-1} (Fig. 2 *a*), which are typical for antiparallel β-sheet formation. When TTR (5 μM, pH 5) is heated to 85°C and the light scattering is recorded, we notice a 15-fold increase in the scattered light intensity, suggesting its aggregation (data not shown). Thus, we assigned these two latter bands to nonnative, aggregated β-sheets. Probably, upon heating, the protein loses its internal β-sheet contacts to establish new interchain contacts, which result in its aggregation. Besides the appearance of these nonnative β-sheets upon heating, the band related to random-coil structures (1646 cm^{-1}) decreases instead of increasing with heating, suggesting that the random structures are being reorganized into another secondary-structure element to be incorporated into these aggregates. Thus, we can conclude that within the heat-induced aggregates, TTR has a partially folded conformation, since elements of secondary structure are still present.

A very similar profile is observed for the temperature-induced unfolding of TTR at pD 7.5 (not shown), although the extent of nonnative, aggregated β-sheet formation upon heating is less pronounced than at pD 5.0 (22% vs. 15.3%). The decrease in random-coil content upon thermal denaturation was similar at both pDs (from 30% at 25°C to 21% (±2%) at 98°C). Upon cooling from 98°C to room temperature at both pDs (Fig. 2 *a*), the IR spectrum 18 h after cooling is completely different from the one observed at 25°C before heating, demonstrating that the denaturation followed by the aggregation of the protein is irreversible (as indicated by the isolated symbols at the *right* in Fig. 2 *b*).

If we compare the percentage of β-sheet structure after cooling to 25°C, it is higher at pD 5.0 than at pD 7.5 (28.3% at pD 5 vs. 19.2% at pD 7.5, see also Table 2). This result is compatible with the greater tendency of TTR to undergo aggregation at acidic pH. Since TTR can form amyloid fibrils at acidic pH as seen by AFM and transmission electron microscopy (41), these aggregates formed after the heat denaturation of TTR might have a fibrillar structure. However, as will be discussed later (see Fig. 5), the IR spectrum of the amyloid fibril of TTR produced at pH 4.4 is completely different from the one observed at high temperatures or at 25°C after cooling down. Thus, as expected, the aggregates formed upon heating are probably not ordered. Another important observation derived from the thermal-induced unfolding of wt TTR is its great thermal stability: the secondary structure of TTR remains almost unchanged up to 80°C (Fig. 2 *b*), where most of the proteins have already lost their structures. As reported by Shnyrov and collaborators (22), the thermal denaturation transition of wt TTR as studied by differential scanning calorimetry occurs at 101.7°C, indicating its impressive thermal stability.

Indeed, previous thermodynamic studies where urea or guanidine hydrochloride were used as perturbing agents have already revealed the great stability of TTR, where long incubation times (72–96 h) are necessary for complete dissociation-denaturation of the protein as followed by the changes in tryptophan fluorescence or by tetramer dissociation. However, in these studies, changes in the secondary-structure content of TTR were not evaluated (18,19,33).

High hydrostatic pressure-induced denaturation of TTR as followed by FTIR

In previous high-pressure studies performed by our group with TTR, we have used tryptophan emission as a sensor of the tertiary-structure content of TTR under pressure (28,29). The changes in the chemical shift of the tryptophan εH at 9.95 ppm were also used as probe in the high-pressure NMR study performed by Niraula and collaborators (14). In all these studies, most of the spectroscopic changes took place in a pressure range of 2–3 kbar.

With a view to obtaining a complete description of the secondary structural alterations that occur with TTR under pressure and after pressure release, we now use high-pressure FTIR and a diamond anvil cell, which allows measurements up to 12 kbar. The experiments were performed at pD 7.5 and 5.0 at two temperatures, 37°C (Fig. 3) and 5°C (Fig. 4).

As seen in Fig. 3, where pressure was applied at 37°C at pD 7.5 (*panels a* and *b*) or at pD 5.0 (*panel c*), the pressure-induced unfolding occurs with a $p_{1/2}$ value (the pressure that causes 50% unfolding) of 3.4 (±0.1) kbar (with an onset of unfolding at $p = 3.3$ (±0.3) kbar) at pD 7.5 and of 3.1 (±0.1) kbar (with an onset of unfolding at $p = 2.9$ (±0.3) kbar) at pD 5.0 and is indicated by significant changes in the amide I′ band region: The intensity of the main peak due to the β-sheet structure (at ~1628 cm^{-1}) decreases (Fig. 3, *b* and *c*, *solid triangles*) and, concomitantly, there is an increase in the peak related to disordered structures (at ~1645 cm^{-1}) (Fig. 3, *b* and *c*, *open squares*). The increase and blue shift of the 1655-cm^{-1} band to 1658 cm^{-1} after unfolding probably indicates the formation of loops, which absorb in the same wavenumber region as α-helices (35).

Upon pressure-induced unfolding at 37°C, the total amount of β-sheet decreases from 43 to 29 (±2)% at pD 7.5, and from 41 to 26 (±2)% at pD 5.0. The fraction of random coil increases from 26 to 40 (±2)% at pD 7.5, and from 30 to 38 (±2)% at pD 5.0. Note that not all the β-sheet content of TTR is lost under pressure, suggesting retention of part of the secondary structure and formation of a partially unfolded state.

It is worth emphasizing that most of the changes in the maximum emission of the tryptophan residues that take place under pressure also occurred in this pressure range (up to 3.5

TABLE 2 Comparison of the percentage of secondary-structure components of wt TTR obtained from FTIR spectra collected at 25°C, 18 h after high-temperature treatment at 25°C, and 18 h after decompression at the specified temperatures and pD values

Secondary-structure content of wt TTR after various treatments								
	After high-pressure treatment				After high-temperature treatment		Native TTR (soluble)	Acidic fibrils
	pD 5.0		pD 7.5		pD 5.0	pD 7.5	pD 7.5	
Secondary structure (%)	37°C	5°C	37°C	5°C	25°C	25°C	25°C	Incubated at 37°C, pH 4.4
α-Helix	6	11	5	10	1	4	3	10
Random coil	26	38	35	38	23	22	29	14
Turns	22	26	20	27	21	23	23	32
Native β-sheets		25	40	25	27	32	42	0
1625 cm^{-1} β-sheets	46	0	0	0	0	0	0	44
1686/1616 cm^{-1} β-sheets	0	0	0	0	28	19	3	0
All β-sheets	46	25	40	25	55	51	45	44

Also shown for comparison are the percentages of secondary structure of the fibrils produced at atmospheric pressure at 25°C upon acidification. The error is ±2%.

kbar), although at slightly lower pressure values (28,29). The $p_{1/2}$ value extracted from fluorescence measurements (sensor of the tertiary-structure changes) at pH 7.5 was 2.7 kbar. Although there is a large difference in the protein concentration used in those experiments (micromolar for fluorescence measurements versus millimolar in FTIR), which could explain the slight discrepancy in the $p_{1/2}$ values, we did not observe any dependence on protein concentration during pressure-induced dissociation-denaturation of wt TTR by HHP (29). Besides, when denaturation of TTR was evaluated by NMR where the protein concentration used was in the millimolar range, the $p_{1/2}$ value found at pH 7.1, 37°C, was 2.18 bar (14).

Thus, assuming that the dissociation of TTR is not accompanied by concentration dependence as observed for other oligomers (25), we can conclude that the loss of tertiary structure under pressure precedes the partial loss of secondary structure at slightly higher pressures. This behavior suggests the existence of an intermediate species in the equilibrium between the native and the unfolded states of TTR. Indeed, when the binding of bis-ANS (4,4′-dianilino-1,1′-binaphthyl-5,5′-disulfonic acid), a specific probe for partially folded states, was evaluated under pressure (29), we observed extensive binding at pH < 5.6, suggesting that TTR is not completely unfolded under pressure at these pH but instead forms a partially unfolded state. This result suggests that, although at pD 5 and 7.5 the changes in secondary structure under pressure are roughly the same (Figs. 3 and 4), the changes in the tertiary contacts are different. The population of an ''amyloidogenic-prone'' species at high pressure only occurs at pHs below 5.6 (28,29). The explanation for this dependence on pH may reside in the fact that some conformational states (such as molten globules) are favored only at low pH (11–13,16,20).

To ensure that no additional structural changes would occur at higher pressures, we extended the pressure range of investigation at pD 5.0 up to 12 kbar (data not shown). At this elevated pressure, we did not notice any additional change in the amide I′ band: the content of β-sheets at 12 kbar is 27%, whereas it is 30% at 4 kbar. A similar scenario holds for the random-coil structures, which represent 37% of the total secondary structure at 12 kbar and 38% at 4 kbar. However, it is striking that even at this elevated pressure, not all native β-sheet structures of TTR are disrupted by pressure: the protein keeps ~60% of its β-sheet content, which again demonstrates the unusually high thermodynamic stability of TTR.

To see whether low temperatures facilitate the unfolding of TTR, we performed pressure titration curves at 5°C (Fig. 4), at pD 7.5 (Fig. 4, *a* and *b*), and at pD 5.0 (Fig. 4 *c*). At both pD values, the changes in the secondary structure occur in the same pressure range. However, since low temperatures weaken hydrophobic interactions, resulting in protein destabilization (42,43), TTR unfolds at 5°C at lower pressure values than at 37°C. The $p_{1/2}$ values obtained at 5°C were 2.2 (±0.1) kbar at pD 5.0 and 2.4 (±0.1) kbar at pD 7.5. Even at 5°C, the content of β-sheets decreases at pD 7.5 from 45% at atmospheric pressure to 26% at 4 kbar (retention of 58% of all β-sheets), whereas the random-coil content increases from 24% to 37%. The same changes take place at pD 5.0, 5°C: β-sheets decrease from 42% to 25% and random coil increases from 25% to 36% in going from atmospheric pressure to 4 kbar, respectively.

Hence, when we compare the secondary-structure content of TTR at high temperatures with the content at high pressure, we can conclude that TTR generates completely different species: 1), whereas at high temperatures the extent of random-coil structure decreases from 30% to ~20% at 98°C, under pressure, for all conditions investigated here, the extent of random coil always increases (from ~28% to ~37%, depending on the condition); 2), nonnative β-sheets (1686/1616 cm^{-1} bands) increase drastically at high temperatures (20–30%) but remain negligible under pressure and after pressure release; and 3), the percentage of native β-sheet structures decreases only partially at high temperatures and high pressures, suggesting that the β-barrel of TTR is only partially dismantled.

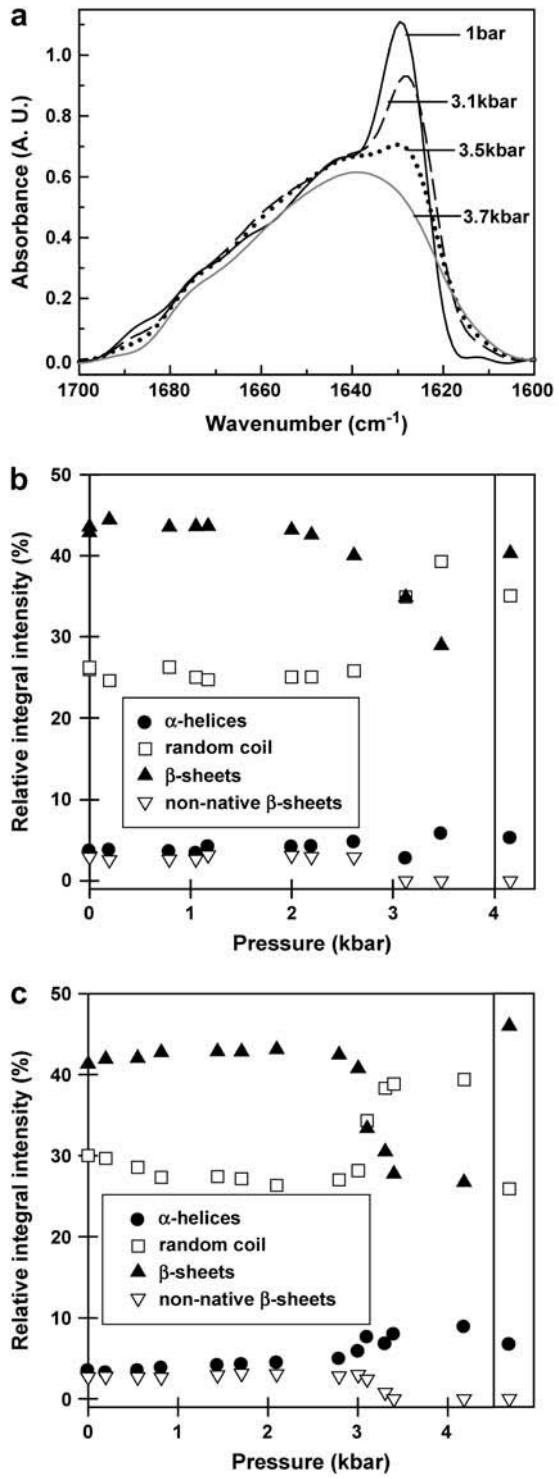

FIGURE 3 High-pressure-induced unfolding of wt TTR at 37°C. (*a*) FTIR spectra of 4% (w/w) wt TTR at pD 7.5 as a function of increasing pressure at 37°C (only selected pressures are shown). Relative intensities of the secondary-structure components as a function of pressure at pD 7.5 (*b*) and at pD 5.0 (*c*). The isolated symbols on the right correspond to the respective secondary-structure components after returning to atmospheric pressure (turns are not shown).

An interesting point to be stressed is that there is an almost constant decrease of ~40% in the content of native β-sheets at 4 kbar, regardless of the pD or temperature employed. This means that ~23 amino acid residues (out of 56 residues involved in A–H strands) are taking on other elements of secondary structure under pressure (mainly random coil and turns). As previously shown by H-D exchange experiments (44,45), the CBEF sheet of TTR is more labile than the other half of the barrel (ADGH) and partially exchanges its H by D. The CBEF sheet has in total 29 amino acid residues. Hence, it is tempting to speculate that this labile region might be the one that is being dismantled upon pressurization. Considering that tryptophan 41, which senses mostly the perturbation in the tertiary structure of TTR upon denaturation, is located in a loop proximal to the C-strand, this residue would also have its maximum emission displaced to the red under pressure, which is indeed observed (28,32).

Comparing the secondary-structure content of the TTR species formed after heat and pressure treatments with that of the fibrillar state

In our previous studies performed with wt and variants of TTR (L55P and V30M), we have shown that after a cycle of compression-decompression at pH 5, 37°C, 3.5 μM TTR, there is a large and fast (<30 min) increase in the light scattering accompanied by thioflavin T and Congo red binding (28,29,46). Altogether, these data suggest that TTR undergoes fibrillogenesis after decompression. It has to be emphasized that the incubation of TTR for several days at atmospheric pressure at pH 5 leads to negligible fibril formation as seen by the changes in absorbance or by thioflavin T binding (11,16); thus the fibrils formed after decompression result from the specific effect of high pressure, which renders the structure of TTR amyloidogenic. Thus, it is reasonable to assume here that the FTIR spectrum obtained after high-pressure treatment at pD 5.0 and 37°C is similar to the one displayed by amyloid fibrils formed at acidic pH.

To pursue this, we collected the FTIR spectrum of TTR fibrils formed by incubating the protein for 3 days at atmospheric pressure at 37°C, pH 4.4, in the presence of KCl and compared it with the spectrum of the 'after-pressure' samples at pD 5 and 7.5 at 37°C (Fig. 5 *a*). We also included in this figure, for comparison, the spectra of the native TTR and of the aggregates produced after heat treatment at pD 5.0. There are clear differences between the spectra of the soluble TTR (*solid black line*) and the one displayed by the acid-induced amyloid fibrils grown at atmospheric pressure (*dotted shaded line*). Interestingly, the spectrum of the sample that was subjected to a cycle of compression-decompression at pD 5.0, 37°C (*dashed line*), where we believe amyloid fibrils are formed, is quite similar to the one displayed by the acid-induced fibrils grown at atmospheric pressure (Fig. 5 *a*).

In both spectra the band at ~1625 cm^{-1}, although broad, is the most prominent, indicating the formation of novel

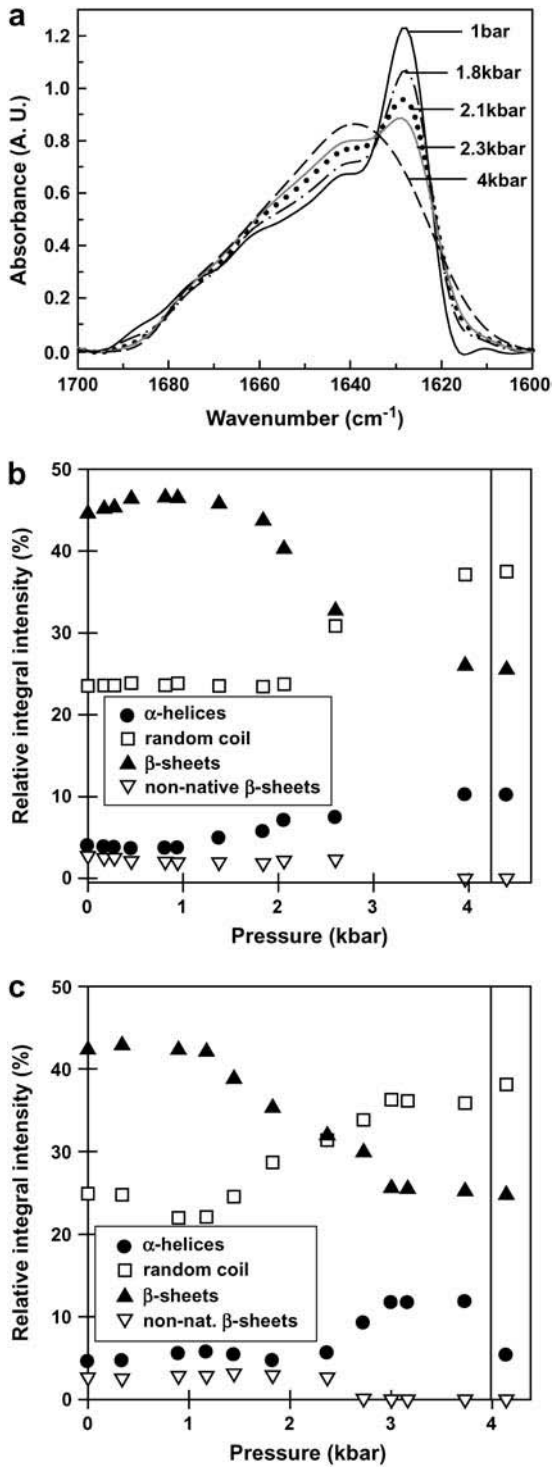

FIGURE 4 High-pressure-induced unfolding of wt TTR at 5°C. (*a*) FTIR spectra of 4% (w/w) wt TTR at pD 7.5 as a function of increasing pressure at 5°C (only selected pressures are shown). (*b*) Relative intensities of the secondary-structure components as a function of pressure at pD 7.5 and at pD 5.0 (*c*). The isolated symbols on the right correspond to the respective secondary-structure component after returning to atmospheric pressure (turns are not shown).

β-sheets contacts, which are different from the ones present in the native protein. Such a band has been observed in the IR spectrum of several amyloid fibrils, including insulin (where it is interpreted as parallel β-sheet structure) and $TTR_{105–115}$, a short peptide derived from TTR (30,47–49). This band, which is characteristic of the amyloid fold, is not observed in the IR spectrum of the sample that was compressed-decompressed at pD 7.5, 37°C (Fig. 5 *a*, *shaded line*). The spectrum of the heat-induced aggregates (*dotted black line*) is completely different from the one displayed by the amyloid fibrils; it has absorption bands at 1616 and 1686 cm^{-1}. This result reinforces our assumption that the heat-induced aggregates have a different, nonamyloidal architecture. The inset in Fig. 5 *a* shows the spectrum obtained immediately after decompression and 18 h after decompression at pD 5, showing that all structural alterations are already present after decompression.

Table 2 presents the percentages of secondary-structure elements calculated from the IR spectra in Fig. 5 *a*. It is interesting to note that the random-coil content of the acidic fibrils grown at atmospheric pressure is considerably lower than that of the soluble protein (14% vs. 29%). The β-sheet content, however, is similar (~43%) in the two species, whereas the content of turns increases in the fibrils (32% vs. 23%). Recently, Olofsson and collaborators (50), by the use of solution NMR spectroscopy in combination with H/D exchange, proposed a model for the organization of the TTR amyloid fibril. Their model suggests a fibril core composed of six β-strands (A-B-E-F-G-H). Strands C and D form a long loop, leaving strands A and B available for intermolecular interactions. This proposal is in accordance with our observations, since most of the native β-strands are preserved in the amyloid fibril of TTR.

Previous studies performed with TTR have shown that the monomeric amyloidogenic intermediate loses part of the β-barrel, suggesting that major structural rearrangements have to take place before amyloidogenesis (32,44,51). However, the data presented here and in the work from Zandomeneghi and collaborators (37) show that the β-sheet content of the fibril is essentially the same as that of the native, soluble state of TTR. An essential difference is found in the alignment of β-strands, the signal of which is located at 1630 cm^{-1} in the native protein, and shifting to 1625 cm^{-1} in the fibrils. Thus, we have to assume that TTR first loses part of the β-sheets in going from a tetramer into a partially folded monomer (amyloidogenic intermediate), but afterward it re-forms the β-sheets as it progresses from the partially folded monomer to the amyloid fibrils. This rearrangement is accompanied by a decrease in random-coil structures and by an increase in the content of turns (Table 2).

Table 2 also presents a detailed description of the secondary-structure content of all species recovered from high-pressure treatments at pD 5 and 7.5, at 5°C and 37°C, respectively. The last line shows that the samples with a β-sheet content closest to that of the acidic fibrils grown at

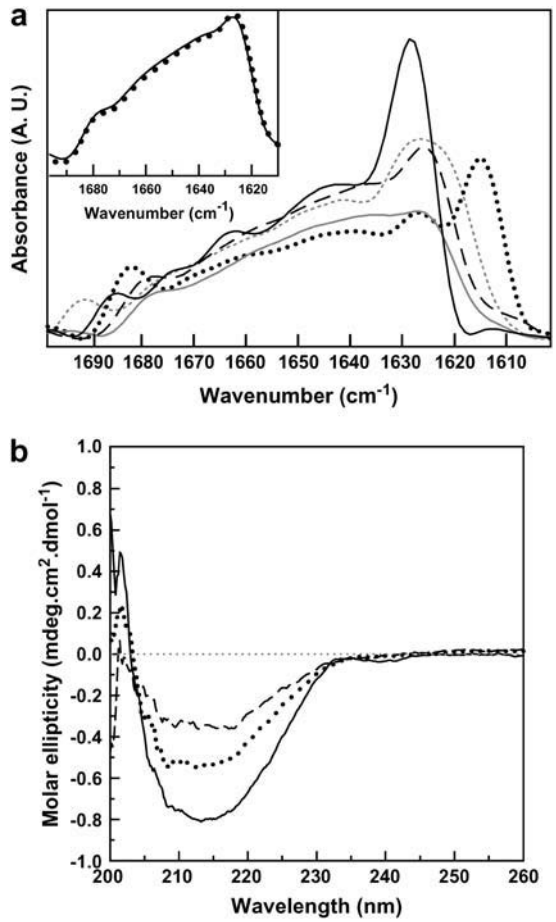

FIGURE 5 Comparing the secondary-structure content of wt TTR after different treatments by FTIR and CD. (*a*) FTIR spectra of 4% w/w TTR in different oligomeric states: native state pD 5.0 (*solid black line*); after heat unfolding at pD 5.0 (*dotted black line*); after decompression at pD 5.0 (*dashed line*); after decompression at pD 7.5 (*solid shaded line*); fibrils of TTR grown at pH 4.4 (*dotted shaded line*). (*Inset*) Comparison between the spectra obtained immediately after decompression at pD 5.0 (*solid line*) and 18 h after returning to atmospheric pressure (*dotted line*). (*b*) CD spectra of 5 μM wt TTR at pH 7.5 (*solid line*), TTR fibrils grown at pH 4.4 (*dotted line*), and of 5 μM TTR incubated at 80°C (*dashed line*).

atmospheric pressure (44%) are the ones that were subjected to a cycle of compression-decompression at 37°C (46% at pD 5.0 and 40% at pD 7.5). When the experiment was performed at 5°C, the amount of β-sheet recovered was even lower (25%) than that of the native protein (45%), suggesting irreversibility of the unfolding process. However, it has to be emphasized that the content of random coil remains elevated (35–38%) in all samples recovered from pressure treatment (Table 2), except for the sample compressed at pD 5.0, 37°C. This suggests that these treatments lead to an incompletely folded protein, which still has some floppy and unstructured segments.

The data presented here are in accordance with our previous work showing that the species recovered from pressure treatment under nonaggregating conditions (named T_4*, which is populated after HHP, for instance, at pH 5 and 1°C) is thermodynamically less stable than the native, noncompressed tetramer (28). Now that we have evaluated the secondary structure of this altered species, it is possible to understand why it is so labile: it has a lower β-sheet and higher random-coil content.

When we analyze the species formed after heat-induced denaturation, the most prominent change is the marked increase in the bands at 1686/1616 cm^{-1} (51–55%), which is absent from the acid-induced fibrils, from the pressure-induced fibrils, and from any other sample recovered from HHP treatment.

Altogether, these data suggest that indeed, after pressure treatment at pD 5, 37°C, TTR undergoes fibrillogenesis, forming fibrils that have secondary-structure content similar to that of the acid-induced amyloid fibrils grown at atmospheric pressure. The major discrepancies observed in secondary-structure content of the 'after-pressure fibrils' compared to the acidic fibrils are a lower percentage of turns (22% vs. 32%, respectively) and a higher percentage of random coil in the 'after-pressure fibrils' (26% vs. 14%). It is possible that the higher percentage of unstructured conformations present in the latter species is due to the fact that these fibrils are immature, so that fine adjustments in structure are still required to achieve the same architecture and packing as in the 3-day-old acidic fibrils. Indeed, recently, Dirix and coworkers showed that there are differences in stability between juvenile and aged amyloid fibrils formed from a fragment of TTR (30), which suggests that fine adjustments to the structure of the amyloid fibrils must take place.

Further studies are being performed to see if aging leads to additional changes in the secondary-structure content of the fibrils produced after pressure treatment at pD 5.0. It is noteworthy that there were no major differences between the spectrum collected from after-pressure samples immediately after decompression (not shown) and the one shown in Fig. 5 *a*, which was collected 18 h after decompression. This suggests that the fibrils formed after decompression were not induced by the long incubation time at pH 5. It has already been shown that at this pH, fibrillization of TTR is very subtle or even absent (11,16,51).

Thus, the FTIR spectrum in the amide I′ band region provides a valuable fingerprint of the soluble versus insoluble forms (fibrils and amorphous aggregates) of TTR, because the vibrational frequency of the amide I′ band sensitively depends on the protein packing. By CD, there is no qualitative difference between the spectra of these three states of TTR (Fig. 5 *b*).

We thank Emerson R. Gonçalves for excellent technical support.

This work was supported by grants from Conselho Nacional de Desenvolvimento Científico e Tecnológico (CNPq), FINEP, Fundação de Amparo a Pesquisa do Estado do Rio de Janeiro (FAPERJ), and Central de Aperfeiçoamento de Pessoal de Nível Superior (CAPES) of Brazil to J.L.S. and D.F., by an international grant from the International Centre for Genetic

Engineering and Biotechnology (ICGEB) to J.L.S., and by a grant from the Deutsche Forschungsgemeinschaft (DFG) to R.W.

REFERENCES

1. Blake, C. C., M. J. Geisow, S. J. Oatley, B. Rerat, and C. Rerat. 1978. Structure of prealbumin: secondary, tertiary and quaternary interactions determined by Fourier refinement at 1.8 Å. *J. Mol. Biol.* 121:339–356.
2. Sousa, M. M., and M. J. Saraiva. 2003. Neurodegeneration in familial amyloid polyneuropathy: from pathology to molecular signaling. *Prog. Neurobiol.* 71:385–400.
3. Robbins, J., and J. E. Rall. 1960. Proteins associated with the thyroid hormones. *Physiol. Rev.* 40:415–489.
4. van Jaarsveld, P., W. T. Branch, J. Robbins, F. J. Morgan, Y. Kanda, and R. E. Canfield. 1973. Polymorphism of Rhesus monkey serum prealbumin. Purification and partial structure. *J. Biol. Chem.* 248:7898–7903.
5. Almeida, M. R., and M. J. Saraiva. 1996. Thyroxine binding to transthyretin (TTR) variants-two variants (TTR Pro 55 and TTR Met 111) with a particularly low binding affinity. *Eur. J. Endocrinol.* 2:226–230.
6. Westermark, P., K. Sletten, B. Johansson, and G. G. Cornwell. 1990. Fibril in senile systemic amyloidosis is derived from normal transthyretin. *Proc. Natl. Acad. Sci. USA.* 87:2843–2845.
7. Connors, L. H., A. M. Richardson, R. Theberge, and C. E. Costello. 2000. Tabulation of transthyretin (TTR) variants as of 1/1/2000. *Amyloid.* 7:54–69.
8. Saraiva, M. J. 2001. Transthyretin mutations in hyperthyroxinemia and amyloid diseases. *Hum. Mutat.* 17:493–503.
9. Benson, M. D. 1989. Familial amyloidotic polyneuropathy. *Trends Neurosci.* 12:88–92.
10. Damas, A. M., and M. J. Saraiva. 2000. TTR amyloidosis-structural features leading to protein aggregation and their implications on therapeutic strategies. *J. Struct. Biol.* 130:290–299.
11. Colon, W., and J. W. Kelly. 1992. Partial denaturation of transthyretin is sufficient for amyloid fibril formation in vitro. *Biochemistry.* 31: 8654–8660.
12. McCutchen, S. L., W. Colon, and J. W. Kelly. 1993. Transthyretin mutation Leu-55-Pro significantly alters tetramer stability and increases amyloidogenicity. *Biochemistry.* 32:12119–12127.
13. McCutchen, S. L., Z. Lai, G. Miroy, J. W. Kelly, and W. Colon. 1995. Comparison of lethal and nonlethal transthyretin variants and their relationship to amyloid disease. *Biochemistry.* 34:13527–13536.
14. Niraula, T. N., K. Haraoka, Y. Ando, H. Li, H. Yamada, and K. Akasaka. 2002. Decreased thermodynamic stability as a crucial factor for familial amyloidotic polyneuropathy. *J. Mol. Biol.* 320:333–342.
15. Sekijima, Y., R. L. Wiseman, R. L. Matteson, P. Hammarstrom, S. R. Miller, A. R. Sawkar, W. E. Balch, and J. W. Kelly. 2005. The biological and chemical basis for tissue-selective amyloid disease. *Cell.* 121:73–85.
16. Lashuel, H. A., Z. Lai, and J. W. Kelly. 1998. Characterization of the transthyretin acid denaturation pathways by analytical ultracentrifugation: implications for wild-type, V30M, and L55P amyloid fibril formation. *Biochemistry.* 37:17851–17864.
17. Zhang, Q., and J. W. Kelly. 2003. Cys10 mixed disulfides make transthyretin more amyloidogenic under mildly acidic conditions. *Biochemistry.* 42:8756–8761.
18. Lai, Z., J. McCulloch, H. A. Lashuel, and J. W. Kelly. 1997. Guanidine hydrochloride-induced denaturation and refolding of transthyretin exhibits a marked hysteresis: equilibria with high kinetic barriers. *Biochemistry.* 36:10230–10239.
19. Jiang, X., C. S. Smith, H. M. Petrassi, P. Hammarstrom, J. T. White, J. C. Sacchettini, and J. W. Kelly. 2001. An engineered transthyretin monomer that is nonamyloidogenic, unless it is partially denatured. *Biochemistry.* 40:11442–11452.
20. Hammarstrom, P., Y. Sekijima, J. T. White, R. L. Wiseman, A. Lim, C. E. Costello, K. Altland, F. Garzuly, H. Budka, and J. W. Kelly. 2003. D18G transthyretin is monomeric, aggregation prone, and not detectable in plasma and cerebrospinal fluid: a prescription for central nervous system amyloidosis? *Biochemistry.* 42:6656–6663.
21. Plaza del Pino, I. M., B. Ibarra-Molero, and J. M. Sanchez-Ruiz. 2000. Lower kinetic limit to protein thermal stability: a proposal regarding protein stability in vivo and its relation with misfolding diseases. *Proteins.* 40:58–70.
22. Shnyrov, V. L., E. Villar, G. G. Zhadan, J. M. Sanchez-Ruiz, A. Quintas, M. J. Saraiva, and R. M. Brito. 2000. Comparative calorimetric study of non-amyloidogenic and amyloidogenic variants of the homotetrameric protein transthyretin. *Biophys. Chem.* 88:61–67.
23. Mozhaev, V. V., K. Heremans, J. Frank, B. Masson, and C. Balny. 1996. High pressure effects on protein structure and function. *Proteins.* 24: 81–91.
24. Balny, C., B. Masson, and K. Heremans. 2002. High pressure effects on biological macromolecules: from structural changes to alteration of cellular processes. *Biochim. Biophys. Acta.* 1595:3–10.
25. Foguel, D., and J. L. Silva. 2004. New insights into the mechanisms of protein misfolding and aggregation in amyloidogenic diseases derived from pressure studies. *Biochemistry.* 43:11361–11370.
26. Torrent, J., S. Marchal, P. Tortora, R. Lange, and C. Balny. 2004. High pressure, an alternative approach to understand protein misfolding diseases. *Cell. Mol. Biol.* 50:377–385.
27. Royer, C. A. 2002. Revisiting volume changes in pressure-induced protein unfolding. *Biochim. Biophys. Acta.* 1595:201–209.
28. Ferrão-Gonzales, A. D., S. O. Souto, J. L. Silva, and D. Foguel. 2000. The preaggregated state of an amyloidogenic protein: hydrostatic pressure converts native transthyretin into the amyloidogenic state. *Proc. Natl. Acad. Sci. USA.* 97:6445–6450.
29. Ferrão-Gonzales, A. D., L. Palmieri, M. Valory, J. L. Silva, H. Lashuel, J. W. Kelly, and D. Foguel. 2003. Hydration and packing are crucial to amyloidogenesis as revealed by pressure studies on transthyretin variants that either protect or worsen amyloid disease. *J. Mol. Biol.* 328:963–974.
30. Dirix, C., F. Meersman, C. E. MacPhee, C. M. Dobson, and K. Heremans. 2005. High hydrostatic pressure dissociates early aggregates of TTR105–115, but not the mature amyloid fibrils. *J. Mol. Biol.* 347:903–909.
31. Cordeiro, Y., J. Kraineva, R. Ravindra, L. M. Lima, M. P. Gomes, D. Foguel, R. Winter, and J. L. Silva. 2004. Hydration and packing effects on prion folding and beta-sheet conversion. High pressure spectroscopy and pressure perturbation calorimetry studies. *J. Biol. Chem.* 279: 32354–32359.
32. Lai, Z., W. Colon, and J. W. Kelly. 1996. The acid-mediated denaturation pathway of transthyretin yields a conformational intermediate that can self-assemble into amyloid. *Biochemistry.* 35:6470–6482.
33. Hammarstrom, P., X. Jiang, A. R. Hurshman, E. T. Powers, and J. W. Kelly. 2002. Sequence-dependent denaturation energetics: a major determinant in amyloid diseases diversity. *Proc. Natl. Acad. Sci. USA.* 99:16427–16432.
34. Panick, G., R. Malessa, and R. Winter. 1999. Differences between the pressure- and temperature-induced denaturation and aggregation of beta-lactoglobulin A, B, and AB monitored by FT-IR spectroscopy and small-angle x-ray scattering. *Biochemistry.* 38:6512–6519.
35. Byler, D. M., and H. Susi. 1986. Examination of the secondary structure of proteins by deconvolved FTIR spectra. *Biopolymers.* 25:469–487.
36. Herberhold, H., S. Marchal, R. Lange, C. H. Scheyhing, R. F. Vogel, and R. Winter. 2003. Characterization of the pressure-induced intermediate and unfolded state of red-shifted green fluorescent protein—a static and kinetic FTIR, UV/VIS and fluorescence spectroscopy study. *J. Mol. Biol.* 330:1153–1164.
37. Zandomeneghi, G., M. R. Krebs, M. G. McCammon, and M. Fandrich. 2004. FTIR reveals structural differences between native beta-sheet proteins and amyloid fibrils. *Protein Sci.* 13:3314–3321.
38. Toniolo, C., and M. Palumbo. 1977. Solid-state infrared absorption spectra and chain arrangement in some synthetic homooligopeptides in the intermolecularly hydrogen-bonded pleated-sheet beta-conformation. *Biopolymers.* 16:219–224.

39. Krimm, S., and J. Bandekar. 1986. Vibrational spectroscopy and conformation of peptides, polypeptides, and proteins. *Adv. Protein Chem.* 38:181–364.

40. Hornberg, A., T. Eneqvist, A. Olofsson, E. Lundgren, and A. E. Sauer-Eriksson. 2000. A comparative analysis of 23 structures of the amyloidogenic protein transthyretin. *J. Mol. Biol.* 302:649–669.

41. Cardoso, I., C. S. Goldsbury, S. A. Muller, V. Olivieri, S. Wirtz, A. M. Damas, U. Aebi, and M. J. Saraiva. 2002. Transthyretin fibrillogenesis entails the assembly of monomers: a molecular model for in vitro assembled transthyretin amyloid-like fibrils. *J. Mol. Biol.* 317:683–695.

42. Privalov, P. L. 1990. Cold denaturation of proteins. *Crit. Rev. Biochem. Mol. Biol.* 25:281–305.

43. Foguel, D., and J. L. Silva. 1994. Cold denaturation of a repressor-operator complex: the role of entropy in protein-DNA recognition. *Proc. Natl. Acad. Sci. USA.* 91:8244–8247.

44. Liu, K., H. S. Cho, D. W. Hoyt, T. N. Nguyen, P. Olds, J. W. Kelly, and D. E. Wemmer. 2000. Deuterium-proton exchange on the native wild-type transthyretin tetramer identifies the stable core of the individual subunits and indicates mobility at the subunit interface. *J. Mol. Biol.* 303:555–565.

45. Liu, K., J. W. Kelly, and D. E. Wemmer. 2002. Native state hydrogen exchange study of suppressor and pathogenic variants of transthyretin. *J. Mol. Biol.* 320:821–832.

46. Foguel, D., M. C. Suarez, A. D. Ferrao-Gonzales, T. C. Porto, L. Palmieri, C. M. Einsiedler, L. R. Andrade, H. A. Lashuel, P. T. Lansbury, J. W. Kelly, and J. L. Silva. 2003. Dissociation of amyloid fibrils of alpha-synuclein and transthyretin by pressure reveals their reversible nature and the formation of water-excluded cavities. *Proc. Natl. Acad. Sci. USA.* 100:9831–9836.

47. Dzwolak, W., M. Kato, and Y. Tanigushi. 2002. Fourier transform infrared spectroscopy in high-pressure studies on proteins. *Biochim. Biophys. Acta.* 1595:131–144.

48. Bouchard, M., J. Zurdo, E. J. Nettleton, C. M. Dobson, and C. V. Robinson. 2000. Formation of insulin amyloid fibrils followed by FTIR simultaneously with CD and electron microscopy. *Protein Sci.* 9:1960–1967.

49. Dwolak, W., R. Ravindra, J. Lendermann, and R. Winter. 2003. Aggregation of bovine insulin probed by DSC/PPC calorimetry and FTIR spectroscopy. *Biochemistry.* 42:11347–11355.

50. Olofsson, A., J. H. Ippel, S. S. Wijmenga, E. Lundgren, and A. Ohman. 2004. Probing solvent accessibility of transthyretin amyloid by solution NMR spectroscopy. *J. Biol. Chem.* 279:5699–5707.

51. Kelly, J. W., W. Colon, Z. Lai, H. A. Lashuel, J. McCulloch, S. L. McCutchen, G. J. Miroy, and S. A. Peterson. 1997. Transthyretin quaternary and tertiary structural changes facilitate misassembly into amyloid. *Adv. Protein Chem.* 50:161–181.